Applied Energy 327 (2022) 120064

Contents lists available at ScienceDirect

Applied Energy

journal homepage: www.elsevier.com/locate/apenergy

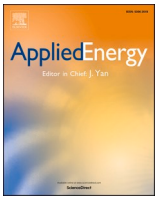

Performance enhancement of phase change materials in triplex-tube latent heat energy storage system using novel fin configurations

Peiliang Yan [a], Weijun Fan [a], Yan Yang [b,*], Hongbing Ding [c], Adeel Arshad [d], Chuang Wen [e,*]

[a] School of Energy and Power Engineering, Beihang University, Beijing 100191, China
[b] School of Petroleum Engineering, Changzhou University, Changzhou 213164, China
[c] School of Electrical and Information Engineering, Tianjin University, Tianjin 300072, China
[d] Department of Mechanical and Construction Engineering, Faculty of Engineering and Environment, Northumbria University, Newcastle upon Tyne NE1 8ST, United Kingdom
[e] Faculty of Environment, Science and Economy, University of Exeter, Exeter EX4 4QF, United Kingdom

HIGHLIGHTS

- Novel fin configurations to enhance phase change material charging performance.
- Efficient melting performance is achieved in thermal energy storage systems.
- Effect of fin structures on PCM melting performance was analysed.
- PCM melting performance is improved by 66% with the novel fin configurations.

ARTICLE INFO

Keywords:
Energy storage
Phase change material
Thermal energy storage
Melting performance
Fin configuration
PCM

ABSTRACT

Phase change material (PCM) has promising applications as an energy storage material in thermal energy storage (TES) systems. However, the low thermal conductivity of PCM limits its applications. To reduce the response time of TES systems, various configurations of fins are used to improve the heat transfer performance of PCM. The Y-structured fins utilize the Y-structure, a common structure in nature, and this study investigates the different structures of Y-shaped fins and the effect of HTF on melting time. A numerical research method based on the enthalpy-porosity method is adopted used for the study. The numerical model of the study is validated using previous experimental data. The simulation results have been obtained, including solid–liquid interface contours, isotherm contours, and evolution of the PCM liquid fraction. The results show that the melting process of the PCM is divided into three main stages and integrated solid fins within the PCM effectively reduce the melting time. Under certain operating conditions, reducing the fin thickness, increasing the fin angle, and increasing the HTF temperature can effectively reduce the PCM melting time. Transient heat transfer rates and dimensionless quantities are analyzed based on numerical results. This study provides potential applications of novel fin structures for new industrial products related to thermal energy storage and management.

1. Introduction

The most significant source of energy for humans is fossil fuels, such as coal, oil and natural gas, the use of which has driven the progress of human civilization since industrialization. However, due to the non-renewable characteristics of fossil fuels, their reserves are now being gradually depleted. The exploitation of renewable energies has become one of the current research hotspots. Solar energy is a clean, renewable source of energy that has been heavily promoted in the industry due to its wide distribution and pollution-free characteristics.

One of the main methods of utilizing solar energy is to convert it into thermal energy for use. However, its application is limited by the natural environment such as circadian and weather conditions. Efficient energy storage is an essential research objective for solar energy consumption. In the thermal industry, thermal energy storage (TES) has received wide attention from researchers as an essential solution for managing the balance between energy supply and energy demand [1]. In particular,

* Corresponding authors.
E-mail addresses: yanyang2021@outlook.com (Y. Yang), c.wen@exeter.ac.uk (C. Wen).

https://doi.org/10.1016/j.apenergy.2022.120064
Received 18 April 2022; Received in revised form 23 September 2022; Accepted 26 September 2022
Available online 7 October 2022

Nomenclature

$a/b/w$	fin length [m]
C	model constants
c_p	specific heat capacity at constant pressure [J/kg.K]
Fo	Fourier number
g	gravity constant [m/s^2]
H	latent heat [J/kg]
k	thermal conductivity [W/m.K]
L	total fin length [m]
$\acute{L}$	non-dimensional number for fin length
p	pressure [Pa]
R_h	hydraulic radius [m]
r_1	inner radius [m]
r_2	outer radius [m]
S_{fin}	fin surface area [m^2]
S_{tube}	annular surface area [m^2]
T	temperature [K]
T_{HTF}	heat transfer fluid temperature [K]
T_l	liquidus temperature [K]
T_m	melting temperature [K]
T_{ref}	reference temperature [K]
T_s	solidus temperature [K]
t	time [s]
t_m	melting time [s]
t_{ref}	finless case melting time [s]
u	fluid velocity in x direction [m/s]
v	fluid velocity in y direction [m/s]

Greek symbols

β	thermal expansion coefficient [1/K]
ε	model constants
θ'	non-dimensional fin angle
θ	fin angle [°]
θ_{ref}	finless case fin angle [°]
λ	local liquid fraction
μ	dynamic viscosity [Pa.s]
ρ	density [kg/m^3]
φ	fin surface area fraction

Subscripts

HTF	heat transfer fluid
PCM	phase change material
TES	thermal energy storage

phase change material (PCM), a kind of low price and stable performance material, has a higher thermal energy density per unit volume/mass than other heat storage materials, and is suitable for various engineering applications across a wide temperature range. It is widely used not only in the field of solar thermal storage [2], but also in a photovoltaic-thermal system [3], building windows [4], building walls [5], air conditioners [6], unmanned underwater vehicles [7], and thermal management [8,9].

However, PCM suffers from low thermal conductivity, severely affecting its response time and limiting its applications. PCM materials are used in double-tube TES systems traditionally, whereas triplex-tube TES systems can provide a larger heat transfer area and increase the melting rate. This system consists of three concentric copper tubes with heat transfer fluid (HTF) flowing through the inner and outer tubes. The remaining annular space in the two tubes is filled by the PCM. Some studies have ignored the effect of natural convection on heat transfer [10], but for most cases this triplex-tube TES system is installed horizontally, making natural convection play an important role in the heat transfer process.

In a triplex-tube TES system, the melting rate of the PCM material determines the application requirements. The melting rate of the PCM is influenced by the HTF, such as the mass flow rate of the HTF, type of HTF, and the inlet temperature of the HTF [11]. Moreover, the material used in the production of the TES system will influence the entire heat exchange process. In addition, the thermal conductivity of the PCM in the tube is a very important influence on the PCM melting rate.

To improve the thermal conductivity of PCM in TES systems, researchers have developed several methods. Examples include adding fins [12], inserting heat pipes [13], adding nanoparticles [14–16] and adding metallic foams [17–19]. Compared to other methods, the method of using fins to increase the heat transfer area is not only easier to install, but also reduces the difficulty of maintaining the system later, making it the most popular method for engineering applications.

There are two main ideas centred on optimizing the thermal conductivity of the fins, minimizing the amount of material and increasing the contact area of the intended component [20]. To enhance the thermal conductivity of PCM, researchers have designed various shapes of fins, such as linear fins [21], the combined fractal fins [22], helical fins [23], tee fins [24], L-shaped fins [25], longitudinal with horizontal fins [26], triangular fins [27], and Y-shaped fins [28]. The application of numerical simulation methods in recent years has greatly contributed to the output of such research. The suitable fin structure has proven to be a massive contributor to heat transfer and the continuous search for new fin structures is a constant goal for researchers.

Many studies of fin construction are focused on fixed forms of fins [29,30], but the fact is that different geometries of the same form of fins can also have a significant impact on the heat transfer performance. Sheikholeslami et al. [31] studied the influence of different angles of V-shaped fins on heat transfer, simulation results showed that discharging rate augments with the rise of the angle of V-shaped fins. Deng et al. [32] tried placing two fins below the horizontal tube and analysed the effect of the arrangement on heat transfer. Mahdi et al. [33] investigated by arranging multiple fins underneath the horizontal tube. For complex fins, Sciacovelli et al. [28] optimized the angle of the Y-shaped fins regardless of natural convection. Yao and Huang [34] optimized the fin width on a new type of triangular fin. The results of the researchers' optimization of complex fins showed that the effort was very valuable. In addition, changing the arrangement of the fins [35] and the position of the inner tubes [36] has been proven to be an effective method of increasing the heat transfer rate.

This paper includes the following novel contributions. Firstly, Y-shaped fins have been proven to be effective in promoting heat transfer. But Y-shaped fins have not been used to enhance the melting of phase change materials (PCM) in triplex-tube latent heat energy storage systems in previous studies. This study analyses the enhancement of the melting process provided by the novel Y-shaped fins. In addition, as the structural parameters of Y-shaped fins are more complex compared to straight fins, the effect of different parameters on the heat transfer performance is analysed using the control variates method in a triplex-tube latent heat energy storage system. Complex-shaped fins may enable future products to put into industrial applications to perform even better.

2. Numerical approach of PCM energy storage system

2.1. Physical model

Fig. 1 (a) shows a cross-section of the triplex-tube TES system with Y-shaped fins used in this study. The heat exchanger is 500 mm in length and is placed horizontally. The TES system consists of three concentric

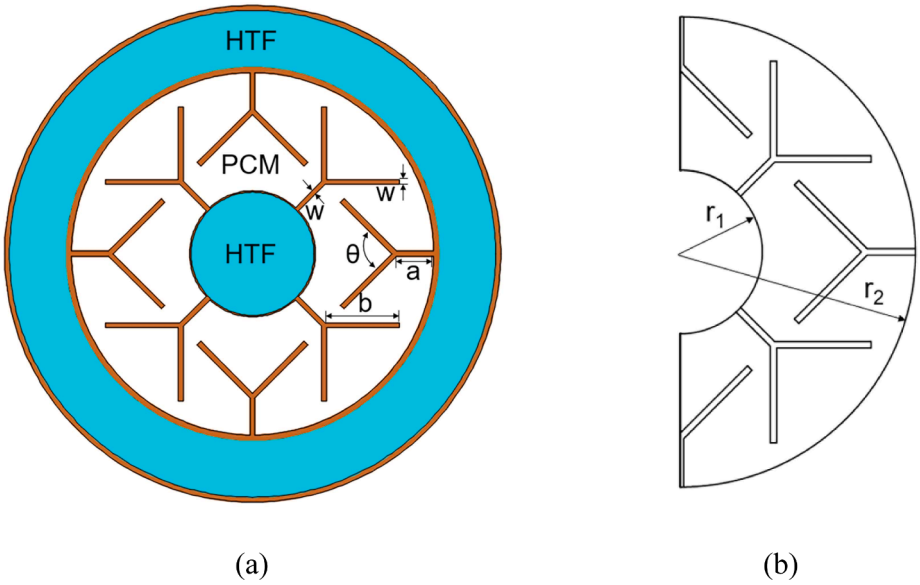

Fig. 1. Two-dimensional view of the triplex tube: (a) the physical domain and (b) the computational domain.

copper tubes with diameters of 50.8, 150 and 200 mm for the inner, middle, and outer tubes respectively. The thickness of both the middle and outer tubes of the TES system is 2 mm, while the thickness of the inner tube is 1.2 mm. The three flow channels of the TES system are filled with HTF, PCM and HTF from the outside to the inside, respectively. The PCM material for this study is RT82 and the HTF is water. Not only does the RT82 material have no super cooling effect, but it also has an almost infinite lifetime and is therefore used as the PCM material for this study. The thermophysical properties of RT82 are mentioned in Table 1 [37]. The Y-shaped fins are placed evenly in the tubes and the detailed dimensions of the fins are provided in Table 2. The fin cross-sectional area remains consistent in all cases in this study. The fin surface area fraction (φ) is adopted as 0.02 because such a ratio has shown good results in previous studies [19]. The Y-shaped structure is common in nature [38] and its application is expected to improve the heat transfer effect. The computational domain for this study is shown in Fig. 1 (b). To save computational resources, half of the pipe cross-section is used as the computational domain in this study, considering the gravity and natural convection effects.

2.2. Governing equations and assumptions

In this study, an enthalpy-porosity model is adopted, which is widely used to simulate PCM melting processes [11]. The model considers the phase change region as porous and the local liquid fraction of the PCM is considered to be equal to the porosity. At a porosity of 0, the material is solid and at a porosity of 1, the material is liquid.

In the enthalpy-porosity model, the equations governing the fluid motion and temperature distribution in the tube are governed by the following equations:

Table 1
The thermophysical properties of the PCM and fins [37].

Property	RT82	Copper
ρ [kg/m^3]	770	8920
c_p [J/kg.K]	2000	381
k [W/m.K]	0.2	387.6
μ [Pa.s]	0.03499	–
H [J/kg]	176,000	–
T_s [K]	350.15	–
T_l [K]	358.15	–
β [1/K]	0.001	–

Table 2
The geometrical dimensions of the computational domain.

Case #	a (mm)	b (mm)	w (mm)	θ (°)	T_{HTF} (K)
1	15.44	30.88	0.5	30	363
2	15.44	30.88	0.5	60	363
3	15.44	30.88	0.5	90	363
4	7.72	15.44	1	90	363
5	3.86	7.72	2	90	363
6	7.72	15.44	1	30	363
7	7.72	15.44	1	60	363
8	3.86	7.72	2	30	363
9	3.86	7.72	2	60	363
10	15.44	30.88	0.5	30	368
11	15.44	30.88	0.5	60	368
12	15.44	30.88	0.5	90	368
13	15.44	30.88	0.5	30	373
14	15.44	30.88	0.5	60	373
15	15.44	30.88	0.5	90	373

Continuity equation:

$$\frac{\partial \rho}{\partial t}+\frac{\partial(\rho u)}{\partial x}+\frac{\partial(\rho v)}{\partial y}=0 \tag{1}$$

Momentum equations:

$$\frac{\partial(\rho u)}{\partial t}+\frac{\partial(\rho u u)}{\partial x}+\frac{\partial(\rho v u)}{\partial y}=-\frac{\partial p}{\partial x}+\frac{\partial}{\partial x}\left(\mu \frac{\partial u}{\partial x}\right)+\frac{\partial}{\partial y}\left(\mu \frac{\partial u}{\partial y}\right)+uA \tag{2}$$

$$\frac{\partial(\rho v)}{\partial t}+\frac{\partial(\rho u v)}{\partial x}+\frac{\partial(\rho v v)}{\partial y}=-\frac{\partial p}{\partial y}+\frac{\partial}{\partial x}\left(\mu \frac{\partial v}{\partial x}\right)+\frac{\partial}{\partial y}\left(\mu \frac{\partial v}{\partial y}\right)+vA+\rho g \beta(T-T_m) \tag{3}$$

where A can be calculated by porosity function [39].

$$A=-C\frac{(1-\lambda)^2}{\lambda^3+\varepsilon} \tag{4}$$

where λ is the liquid fraction during the melting process of the PCM, which can be defined.

$$\lambda=\begin{cases}0 & , \ T<T_s \\ (T-T_s)/(T_l-T_s) & , \ T_s<T<T_l \\ 1 & , \ T>T_l\end{cases} \tag{5}$$

where C is the mushy zone constant, which is used to control damping

and is set here as $C = 10^6$ kg/s.m^3, ε is a minimal value, used to prevent the denominator from reaching 0, here it is set as $\varepsilon = 0.001$.

Energy equation:

$$\frac{\partial(\rho h)}{\partial t}+\frac{\partial(\rho u h)}{\partial x}+\frac{\partial(\rho v h)}{\partial y}=\frac{\partial}{\partial x}\left(k\frac{\partial T}{\partial x}\right)+\frac{\partial}{\partial y}\left(k\frac{\partial T}{\partial y}\right) \tag{6}$$

where h is defined as follows:

$$h=\begin{cases}\int_{T_{ref}}^{T} c_p dT & , \ T<T_s \\ \int_{T_{ref}}^{T_s} c_p dT+\lambda H & , \ T_s<T<T_l \\ \int_{T_{ref}}^{T_s} c_p dT+H+\int_{T_l}^{T} c_p dT & , \ T>T_l\end{cases} \tag{7}$$

where T can be calculated using the following equation [40].

$$T=\lambda(T_l-T_s)+T_s \tag{8}$$

The widths of the fins studied in this paper are equal everywhere and the expression for the area of the fins is,

$$S_{fin}=8w(a+b) \tag{9}$$

The expression for the annular area between the two tubes is,

$$S_{tube}=\pi\left(r_2^2-r_1^2\right) \tag{10}$$

The percentage of fin area is,

$$\varphi=\frac{S_{fin}}{S_{tube}}=\frac{8w(a+b)}{\pi(r_2^2-r_1^2)} \tag{11}$$

The formula for calculating the length dimensionless quantity defined in this paper is,

$$L'=\frac{L}{R_h}=\frac{2(a+2b)}{r_2-r_1} \tag{12}$$

The non-dimensional angle is defined as the ratio of the operating fin angle to the reference angle.

$$\theta'=\frac{\theta}{\theta_{ref}} \tag{13}$$

The Fourier number (Fo) is the ratio of the heat transfer rate to the heat storage rate. In this research, the Fourier number is used to represent the non-dimensional melting time. The reference time is defined as the complete melting time in finless condition. The formula for calculating the Fourier number is,

$$Fo_m=\frac{t_{ref}}{t_m} \tag{14}$$

The following assumptions are used in this study to simplify the research model: (1) liquid-phase PCM flow is transient, laminar and incompressible; (2) temperature change in HTF is negligible; (3) thermophysical properties of the PCM are constant over the operating temperature range and the density of the PCM is governed by the Boussinesq assumption; (4) The volume change, external wall heat loss and radiative heat transfer during the phase change of the PCM are negligible; (5) no-slip condition for velocity presents at the boundary.

2.3. Boundary conditions and simulation methods

In the calculation domain, the initial state temperature of the PCM is 300 K. During the calculation, the temperature of the HTF is constant at 363, 368 and 373 K, respectively. Commercial software ANSYS-Fluent 2022R1 is used for the simulation. The SIMPLE algorithm is adopted for the pressure–velocity coupling and then PRESTO! The scheme is adopted for the pressure correction equation. The detailed procedure of the numerical methodology can be access from the previous reported studies by the author, Arshad, et al. [8].

2.4. Model validation

Three grid schemes with grid numbers 16117, 49,908 and 80,258 have been investigated to predict the variation of liquid fraction with time for the computational domain in the no-fin condition. The calculation time step of 0.3 s is chosen to obtain a stable solution for the investigated working conditions. The results of the calculation are shown in Fig. 2. It can be seen that the computational results for grid number 16,117 are significantly different from those for the other two grid numbers. Considering the computational resources, the case of grid number 49,908 is adopted for this study.

The simulation model in present study was validated using previous reported experimental data from Al-Abidi et al. [41] and the simulation uses the same initial conditions and boundary conditions as the experiment. As can be seen in Fig. 3, the simulation model shows the good agreement with experimental data, indicating that the present model can be used for the study of melting enhancement in the TES system.

3. Results and discussion

Numerical simulation is an efficient tool to analyse the thermal behaviour of phase change materials, which has been widely used in evaluation the melting process [42–44]. A series of numerical simulations are carried out for the TES system studied in this research and results such as isotherms, solid–liquid interface distribution and transient liquid fraction are presented. In this study, the initial state of the entire PCM is all solid, and after being heated from the wall, the entire PCM gradually melts into a liquid. This section describes the phenomena observed.

3.1. Evolution of the solid–liquid interface

A series of numerical studies have been carried out for different cases. The evolution of the solid–liquid cross-section at different stages of the melting process with different angles of the Y-shaped fins is shown in Fig. 4. In the first stage (t < 10 min), the melting structure of the Y-shaped fins is similar. There is a PCM melt layer along the wall surface as well as along the edges of the fins, but the low thickness of the melt layer results in the main heat exchange method being heat conduction. And since the fin temperature decreases as the position to the root increases, the end of the fin melts to a lesser extent. At this time, the angle of the

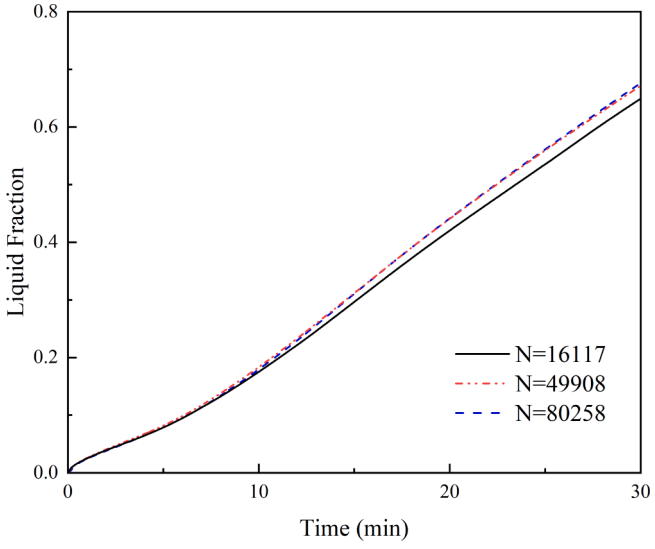

Fig. 2. Grid independences study.

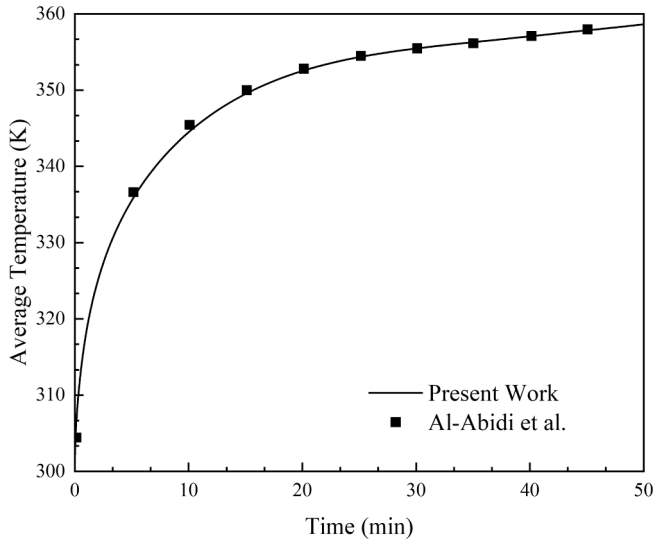

Fig. 3. Comparison of average temperature obtained from present work and experiment data from Al-Abidi et al. [41].

fins has less effect on melting. In the second stage (10 min $< t <$ 30 min), the thickness of the melt layer increases, the solid–liquid interface starts to become deformed, and part of the liquid starts to convert along the area divided by the fins under the influence of buoyancy, this convection movement causes the melting rate to accelerate above the interior of each area divided by the fins. During this stage, the fins effectively transport heat to each zone and prevent any mixing of the individual solid PCMs. In the lower part of the solid PCM, the convective fluid motion impact on the solid PCM causes it to be deformed. The splitting effect becomes more uniform as the angle of the fins increases, and so does the melting rate. As time passes ($t >$ 30 min), the molten liquid gradually increases and occupies most of the space. As the fins still restrict the movement of the solid PCM, it can be found that the remaining solids are still separated by the fins. Due to the low density of the liquid PCM, the buoyancy effect causes the heat fluid to flow in the upper portion of the entire annular channel. The lower half of the solid PCM melts at a slower rate compared to the upper half of the solid PCM while the whole PCM deposits in the lower part of the liquid. The phenomenon remains until the solid is completely melted.

Fig. 5 shows the evolution of the solid–liquid cross-section at different stages of the melting process with different thicknesses of Y-shaped fins. Since the area of the annular space occupied by the fins is fixed, the PCM mass is the same in several cases. The surface area and extension length of the fins vary due to the thickness of the fins, and it can be seen that a 0.5 mm thick fin divides the solid PCM evenly and has the largest heat dissipation area, and therefore melts the PCM completely rapidly. A 2 mm thickness fin not only makes it difficult to conduct heat to the interior of the PCM but with the increased thickness of the melt layer it does not effectively divide the solid PCM, resulting in the main method of heat transfer being heat convection and the fins failing to perform their functions better.

3.2. Distributions of isotherms

Fig. 6 illustrates the isotherm changes for the cases corresponded to Fig. 4. It can be seen that in the first stage, the temperature in each area separated by the fins becomes lower as the distance between the PCM and the fins or wall increases. At this stage, the heat transfer process is dominated by heat conduction. The fins transfer the heat from the walls. At this stage, the internal temperature of the solid PCM rises but melting occurs rarely. The shape of the isotherm begins to change in the next stage, due to the thickening of the melt layer and the convective movement mentioned in section 3.1. As, it can be seen from the isothermal diagram, fluid impingement on a solid-surface leads to the creation of an irregular shape on the surface. In the top and bottom parts of the solid PCM, the contact area between the solid and the liquid increases due to the deformation of the solid surface and the unfinished melting solid extends into the liquid to accelerate the melting process. In the final stage, when the liquid occupies most of the space, thermal convection decreases and the heat transfer process gradually becomes dominated by heat conduction, as can be seen in case 3. There is almost no convective impact isothermal deformation in the bottom of the solids and the PCM solids deposit at the bottom of the space divided by the fins.

Fig. 7 is an isotherm contour corresponding to Fig. 5. When the fin thickness is large, the fins have a limited extension and a large low-temperature zone exists, which remains until the time that case 3 is almost completely melted. Although the internal temperature has increased, the centre of the area does not melt as seen in Fig. 5, demonstrating the effectiveness of the long fins on the splitting of the PCM for heat transfer.

3.3. Effects of fin thickness

The liquid fraction is an important parameter that refers to the percentage of melted PCM liquid to the total PCM. It visually reflects the progress of PCM melting and helps to evaluate the heat transfer in different cases. Fig. 8 shows the evolution of the PCM liquid fraction for different fin thicknesses. In this diagram, each curve goes through three stages, which correspond to the phenomena mentioned in section 3.1. Case 3 achieves the most efficient heat transfer results of the three cases, completely melting the PCM in just 60 min. It is known that when the fin surface area fraction is fixed ($\varphi = 0.02$ in this study), the fin heat dissipation area becomes enlarged as the fin thickness decreases. However, as the local fin temperature decreases with increasing distance from the fin root, the continued decrease in fin thickness does not always obtain a further increase in the melting rate, which suggests that there is a diminishing return on the increase in surface area for heat transfer when designing fins for the industry. Also, compared to the results of Ref. [11], the use of straight fins instead of Y-shaped fins results in a faster melting rate for the fin thicknesses of case 4 as well as case 5, and the melting time for any Y-shaped fin is much less than the melting time required without fins. In addition, Fig. 5 shows that the morphology of the Y-shaped fins prevents them from being able to penetrate the PCM solid better than straight fins. Therefore, when utilizing such type of fins, the total surface area of the fins should be controlled to be larger than the maximum surface area of the straight fins that the heat exchanger can accommodate under the corresponding fin thickness.

3.4. Effects of fin angle

The Y-shaped fins extend into the annular cavity and are obstructive to the liquid flow in the PCM during melting, which affects the thermal transfer to some extent, so the suitable fin angle needs to be investigated. Simulation has been carried out with different fin thicknesses and three different fin angles. The melting process for fins with larger angles has not been investigated as continuing to widen the fin angle would make it impossible to install fins with w = 0.5 mm. The results are shown in Fig. 9, all three graphs show the same trend, that is, the angle of the fins does affect the overall heat transfer rate, but not as much as the thickness of the fins. Also, it is noted that there is a diminishing return on the increase in heat transfer efficiency due to the increase in fin angles. This phenomenon is shown at any fin thickness. It is observed that the heat transfer efficiency increases with increasing fin angle at fin thicknesses of 1 mm and 2 mm, but when the fin thickness is 0.5 mm, the lower solid PCM deposits in the centre of the Y-shaped fins as the fin restricts the flow of liquid PCM. As shown in Fig. 4, the fin temperature at this point is not at the same temperature as the wall, which ultimately causes the melting slower than that in case 2, although the melting in case 3 is faster than that in case 2 for most of the time. This phenomenon suggests

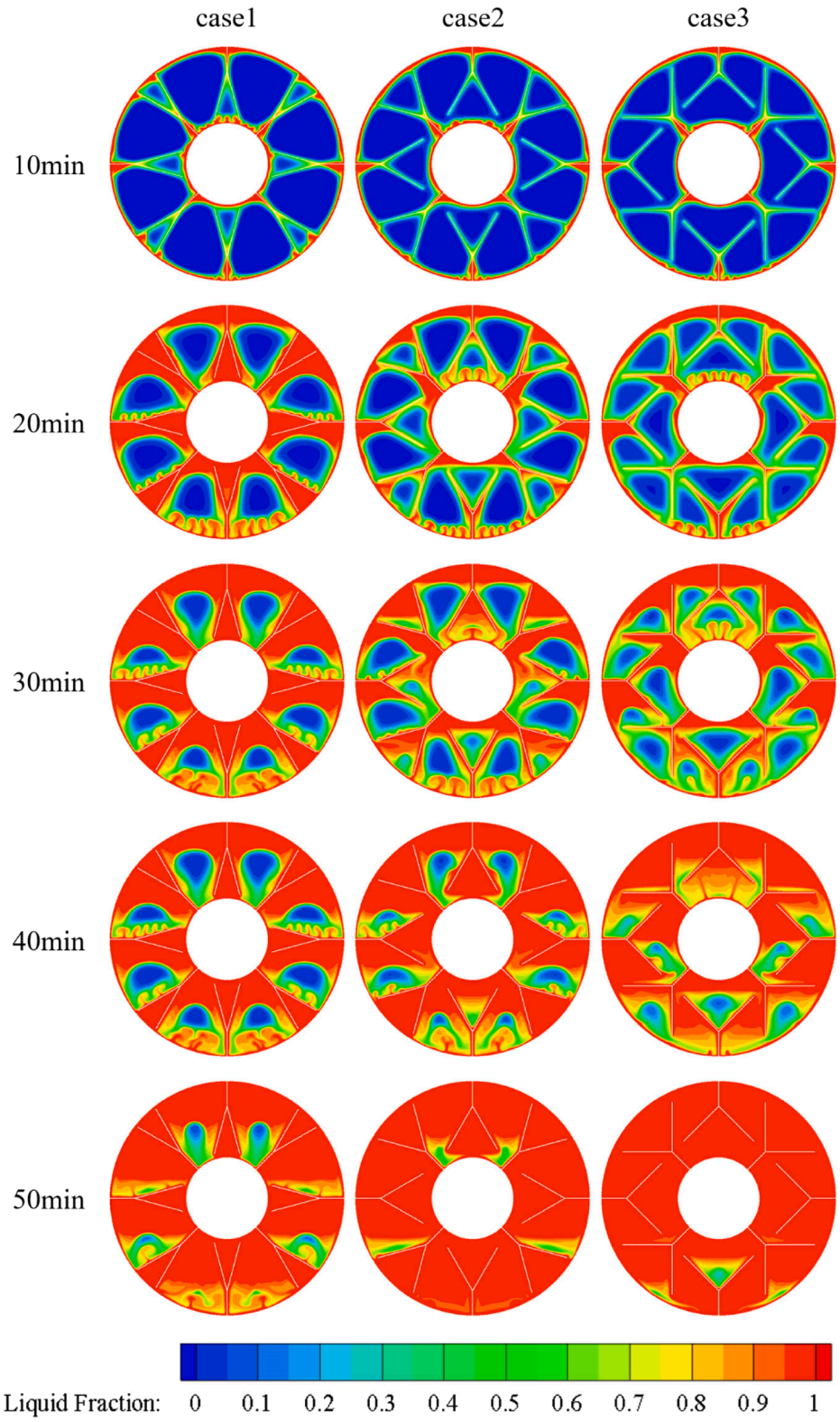

Fig. 4. Contours of the liquid fraction at various fin angles under $w = 0.5$ mm, $T_{HTF} = 363$ K.

that the design of fins should not only consider the partitioning of the PCM by the fins, but also the prevention of solids deposition when installing the fins. To conclude, Table 3 provides a visual representation of the effect of fin angles on melting time. Considering that complete melting without fins takes 162 min [11], the PCM system with the Y-shaped fins requires a minimum of 34.0 % of the time of the original system to achieve complete melting.

3.5. Effects of HTF temperature

An increase in HTF temperature can increase the temperature gradient between the wall or fin and PCM, thus increasing the melting rate. Suitability of the HTF temperature for industrial applications of TES systems will benefit the performance of the system. In the case studied in this section, the effect of HTF temperature on the melting rate

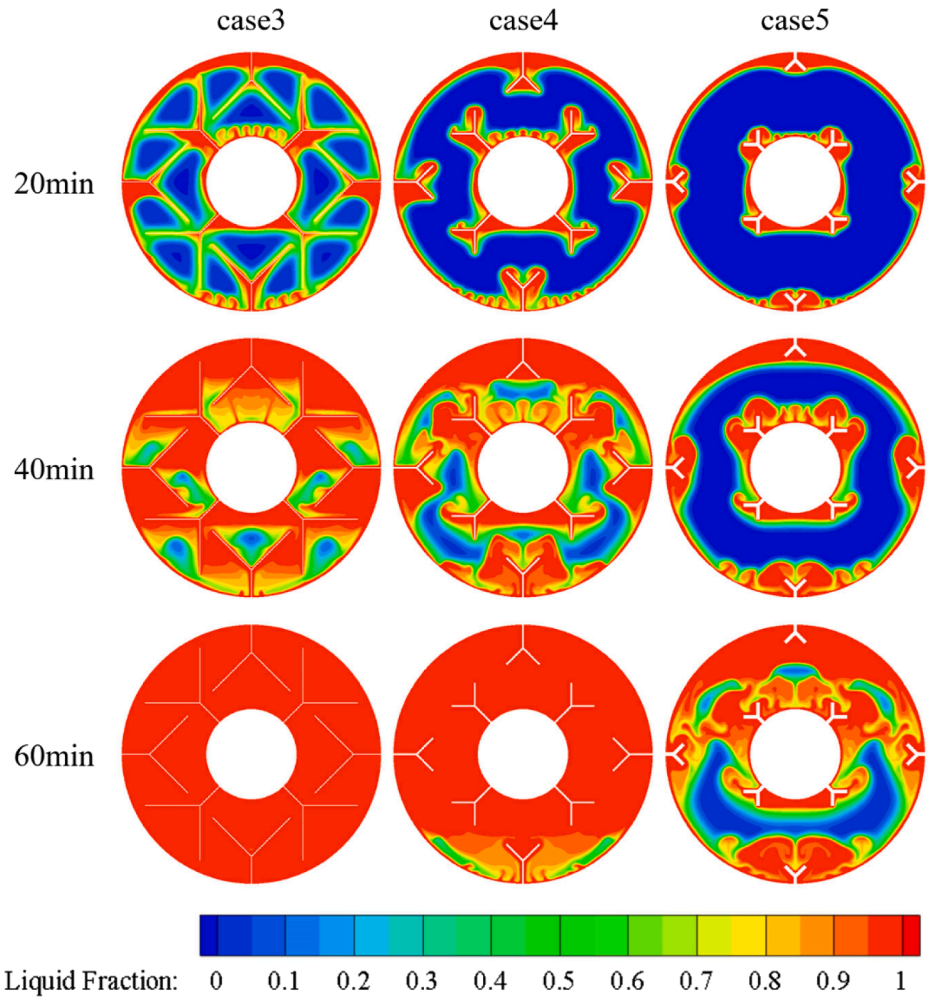

Fig. 5. Contours of the liquid fraction at various fin thicknesses under $\theta = 90°$, $T_{HTF} = 363$ K.

of PCM is analysed at a fin thickness of 0.5 mm. The results can be observed in Fig. 9 (a) as well as in Fig. 10. It can be noticed that the melting rate of the three fin angle cases is found to be similar to the HTF temperature variation, and the effect of the solids deposition phenomenon, mentioned in section 3.4, on the melting rate decreases with the increase of the HTF temperature. The difference in melting time between case 14 and case 15 is only 1 min, which is contributed by the increased temperature gradient. A comparison of the three diagrams also shows that an increase in HTF temperature leads to a faster melting rate, regardless of the operating conditions. However, by increasing the HTF temperature by the same value, the reduction in melting time decreases. In addition, it was observed that changing the HTF temperature had little effect on the working conditions at different angles. The effect of HTF temperature on melting time is shown in Table 4 intuitively.

3.6. Transient heat transfer rates analysis

Fig. 11 shows transient heat transfer rates under different parameters. It is observed that the transient heat transfer rates are gradually decreasing at any given operating condition. In the initial phase, the heat exchange is very intense, which is caused by the direct contact of the PCM solids with the walls and fins. This process lasts for a short time. A liquid PCM film then appears between the heated surface and the solid PCM, and the thermal resistance increases rapidly, resulting in a significant reduction in the transient heat transfer rate. As the liquid phase PCM continues to increase, the thermal convection phenomenon gradually becomes the dominant heat transfer mode, so the rate of heat transfer decreases at this point at a more moderate rate. As the PCM solid becomes progressively smaller and eventually disappears, the heat transfer rate decreases until it approaches zero.

From Fig. 11 (a), it can be seen that the different fin thickness has a very significant effect on the heat transfer rate. In the beginning, the heat transfer rate is much greater for the smaller fin thickness than for the larger fin thickness due to the contact area. This advantage is maintained until the solid disappears and the heat transfer rate tends to zero. In comparison, the angle has very little effect on the heat transfer rate. In Fig. 11 (b), it can be seen that the increase in HTF temperature significantly increases the heat transfer rate and maintains a large heat transfer rate throughout the melting process.

3.7. Dimensionless quantities analysis

The use of the dimensionless method for the structural parameters can provide an intuitive visualisation of the results of the influence of the different parameters on the PCM melting process. The Fourier number is adopted as dimensionless melting time and the melting time of the finless case is set as the reference time. It is capable of calculating the heat exchange time improvement for different structural parameters. The fin length, thickness, angle, and tube diameters are all available for dimensionless analysis. Since the widths of the Y-shaped fins are equal everywhere, the total length of the fins is considered here as the sum of the lengths of the segments. It is worth noting that since the ratio of the cross-sectional area of the fins to the annular cross-sectional area is a fixed value of 0.02 in this study, the dimensionless fin length

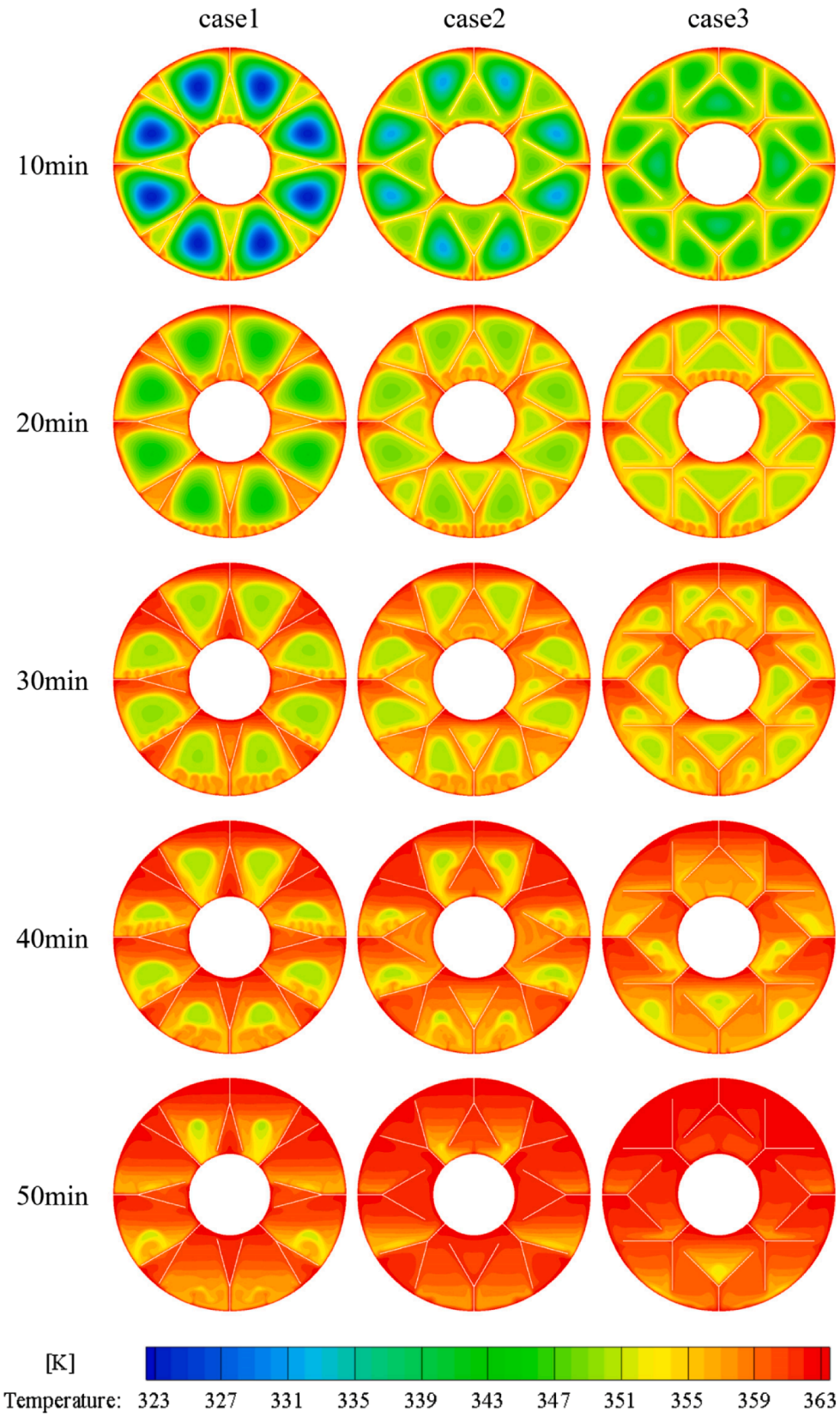

Fig. 6. Isotherm at various fin angles under $w = 0.5$ mm, $T_{HTF} = 363$ K.

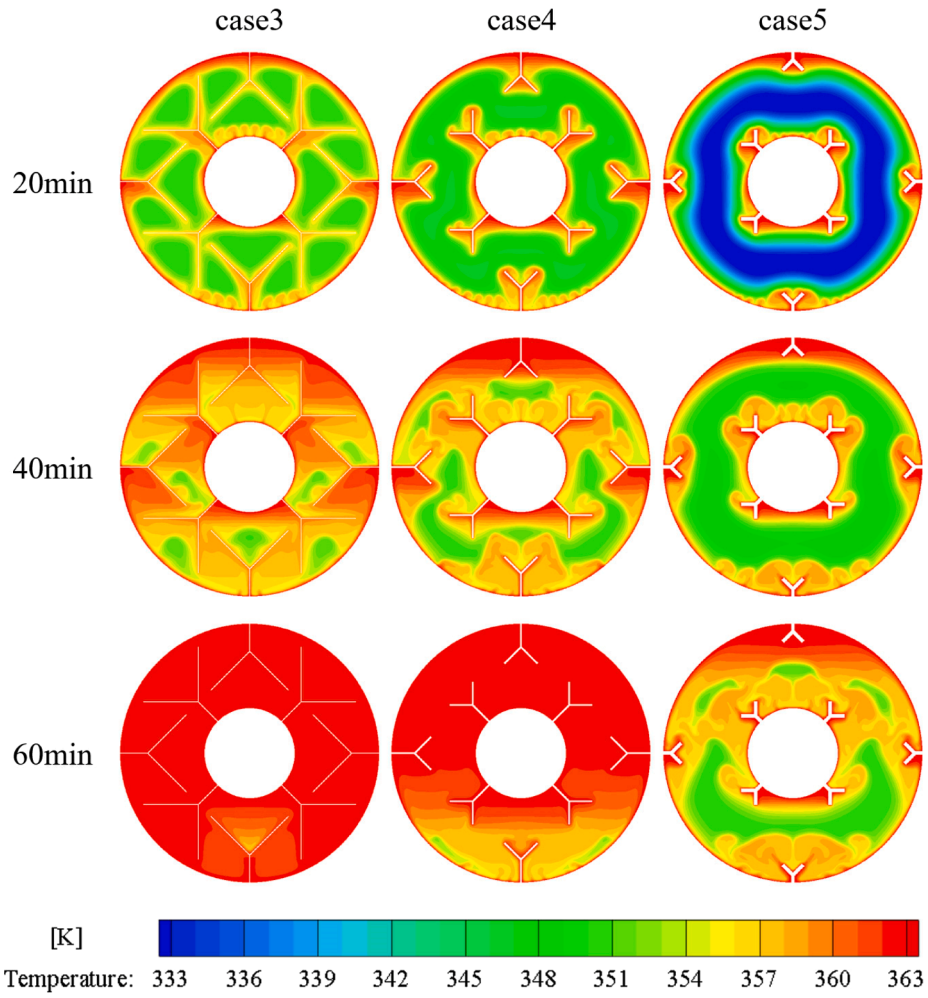

Fig. 7. Isotherm at various fin thicknesses under $\theta = 90°$, $T_{HTF} = 363$ K.

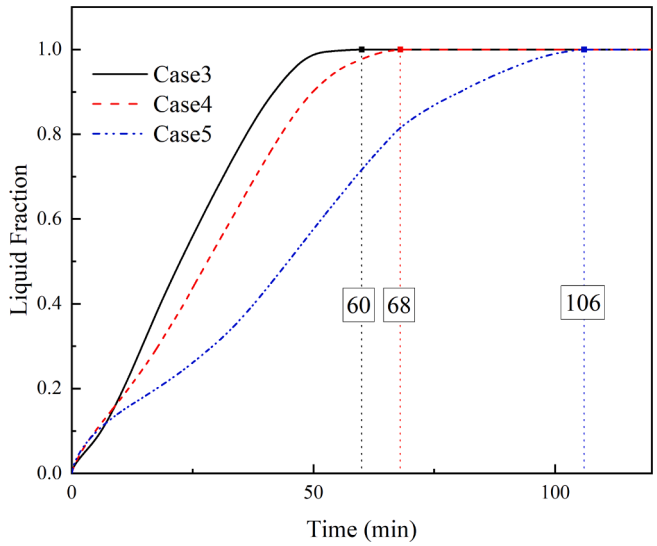

Fig. 8. Evolution of the PCM liquid fraction for different fin thicknesses under $\theta = 90°$, $T_{HTF} = 363$ K.

investigation is the same as the dimensionless fin thickness investigation. In order to take the tube diameters into account in the dimensionless fin lengths, the hydraulic radius is used as the reference fin length. The reference fin angle of dimensionless fin angle is 180°. The dimensionless fin angle can be calculated by Formula 13.

Fig. 12 (a) demonstrates the contribution of dimensionless fin length to the Fourier number (melting time). The fin widths of 2 mm, 1 mm and 0.5 mm correspond to dimensionless fin lengths of 0.81, 1.62 and 3.24, respectively. Fixing other conditions, an increase in the dimensionless length always results in a larger Fourier number, which represents an increase in heat transfer capacity. The increase in fin length not only significantly reduces the melting time, but also provides a visual indication of the diminishing return phenomenon. When the fin angle is at 90° (dimensionless fin angle at 0.5), the deposition of solids severely affects the heat transfer efficiency, making its melt time only higher than that with a fin angle of 60° (dimensionless fin angle at 0.33). Fig. 12 (b) demonstrates the contribution of dimensionless fin angle to the Fourier number for the same fin length. The fin angles of 30°, 60° and 90° correspond to dimensionless fin angles of 0.17, 0.33 and 0.5, respectively. The increase in HTF temperature not only effectively reduces the melting time, but also minimises the effect of deposition of solids, but does not eliminate it. Therefore, case 2 is the best case to achieve a Fourier number of 2.95 (34 % of the reference melting time) without the consideration of HTF temperature, and case 14 is the best case to achieve a Fourier number of 5.4 (18.5 % of the reference melting time) with the consideration of HTF temperature. It can also be found that increasing the HTF temperature by the same volume has approximately the same effect on the Fourier number. Since the Fourier number is the inverse of the ratio of the actual melting time to the reference time, this means that the influence of temperature on the melting time is decreasing.

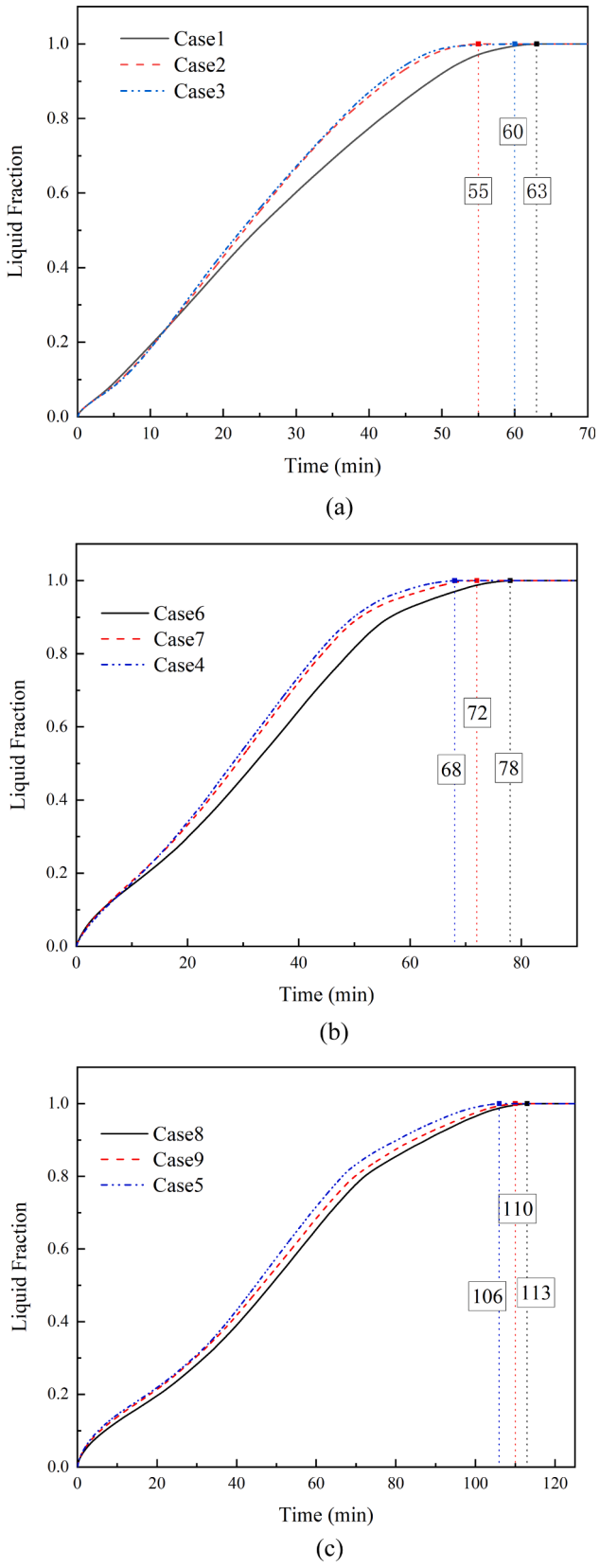

Fig. 9. Evolution of the PCM liquid fraction for different fin angles under T_{HTF} = 363 K (a) w = 0.5 mm; (b) w = 1 mm; (c) w = 2 mm.

Table 3
Effect of fin angles on melting time.

Case #	w (mm)	θ (°)	Melting time (min)
1	0.5	30	63
2	0.5	60	55
3	0.5	90	60
4	1	90	68
5	2	90	106
6	1	30	78
7	1	60	72
8	2	30	113
9	2	60	110

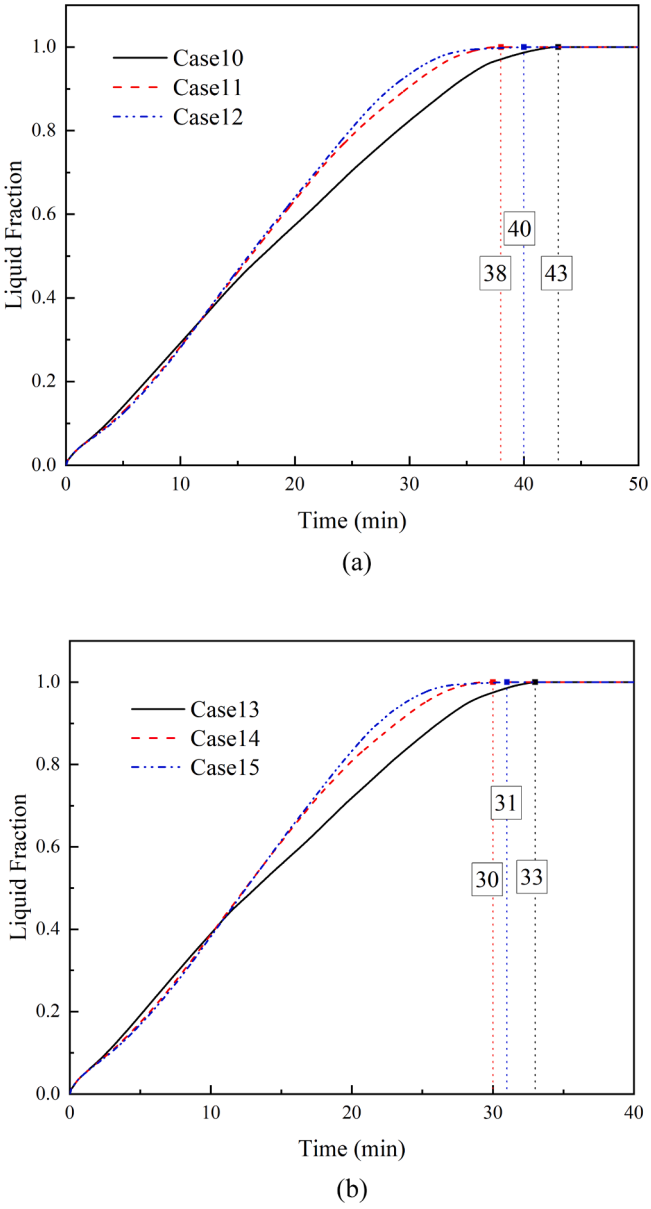

Fig. 10. Evolution of the PCM liquid fraction for different fin angles under w = 0.5 mm (a) T_{HTF} = 368 K; (b) T_{HTF} = 373 K.

4. Conclusions

In this study, Y-shaped fins are brought into the triplex-tube TES storage system, and the melting enhancement of a triplex-tube TES storage system is investigated by analysing the effect of different

Table 4
Effect of HTF temperature on melting time.

Case #	T_{HTF} (K)	θ (°)	Melting time (min)
10	368	30	43
11	368	60	38
12	368	90	40
13	373	30	33
14	373	60	30
15	373	90	31

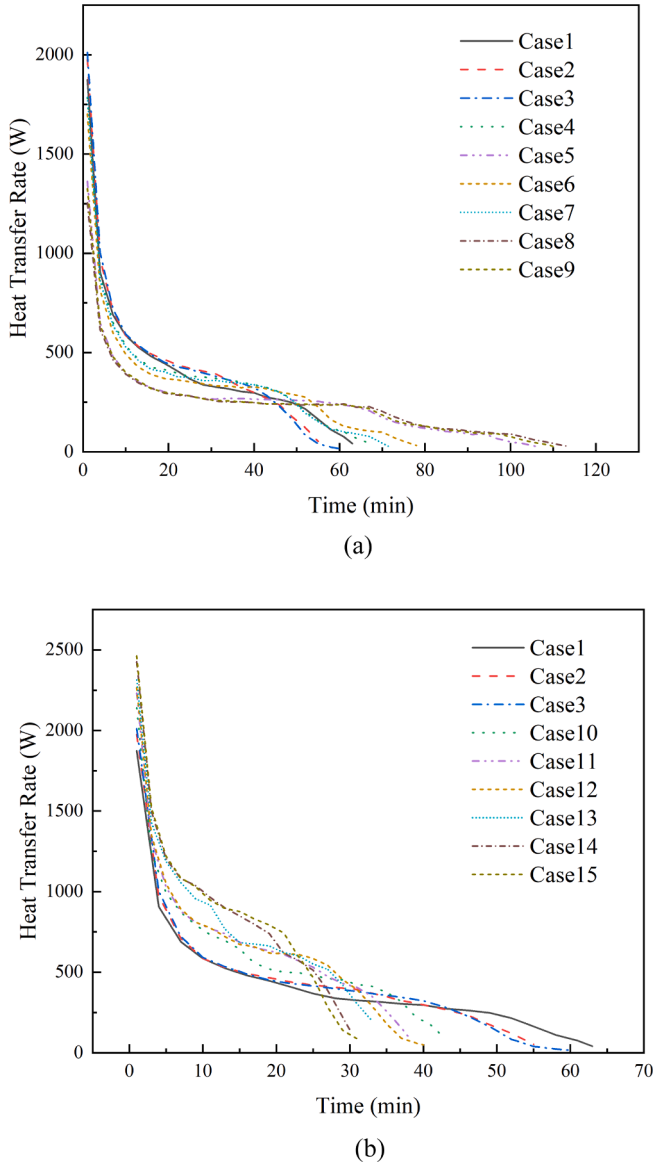

Fig. 11. Transient heat transfer rates under (a) $T_{HTF} = 363$ K; (b) $w = 0.5$ mm.

parameters on the heat transfer performance. This research purpose is to obtain a reasonable morphology for this type of fin and to arrange it in the future TES system. And some conclusions are obtained from the research.

The use of Y-shaped fins effectively facilitates the melting process. With a constant proportion of fins in the cross-section of the triplex-tube system, the melting time decreases with decreasing thickness of the Y-shaped fins. Under the same conditions, an increase in the angle of the fins triggers a more homogeneous division of the PCM solids, which can shorten the melting time. It is also important to prevent the deposition of

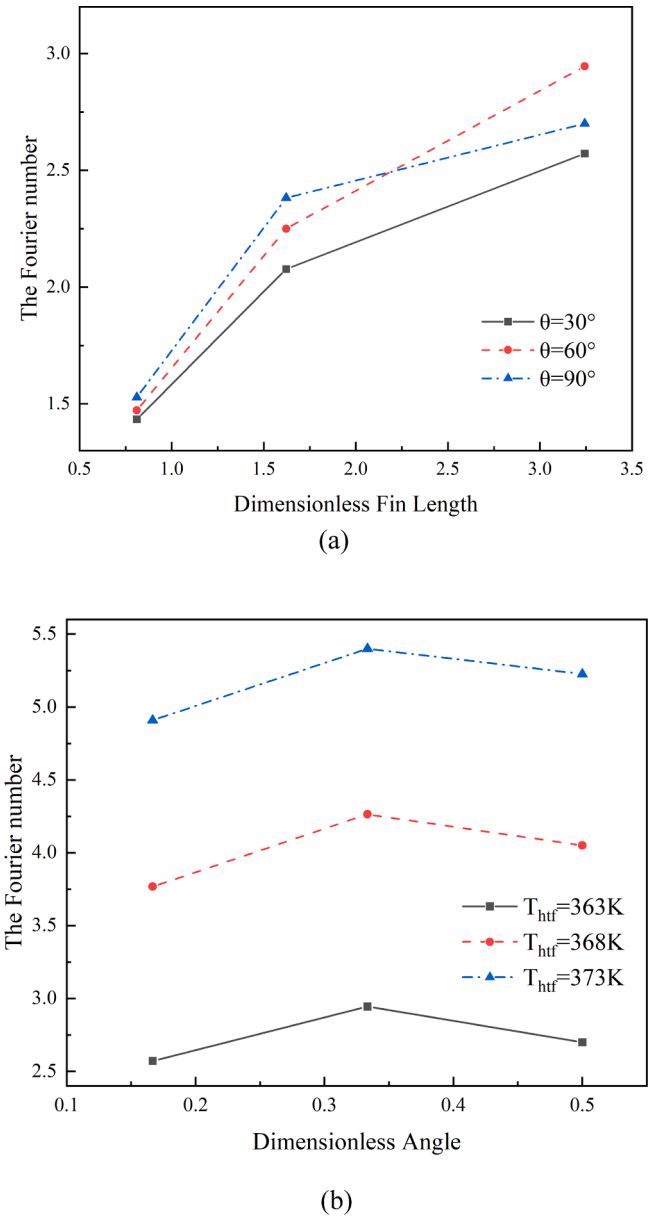

Fig. 12. Contribution of dimensionless quantities to melting time under (a) $T_{HTF} = 363$ K; (b) $w = 0.5$ mm.

solids. Increased HTF temperature helps to reduce PCM melting time. The PCM system with the Y-shaped fins requires a minimum of 34 % of the time of the original system to achieve complete melting.

CRediT authorship contribution statement

Peiliang Yan: Investigation, Discussion, Writing- Original draft preparation and Revising. **Weijun Fan:** Discussion, Reviewing and Revising. **Yan Yang:** Conceptualization, Discussion, Reviewing and Revising. **Hongbing Ding:** Discussion, Reviewing and Revising. **Adeel Arshad:** Discussion, Reviewing and Revising. **Chuang Wen:** Supervision, Conceptualization, Methodology, Investigation, Reviewing and Revising.

Declaration of Competing Interest

The authors declare that they have no known competing financial interests or personal relationships that could have appeared to influence

the work reported in this paper.

Data availability

No data was used for the research described in the article.

References

[1] Chen G, Su Y, Jiang D, Pan L, Li S. An experimental and numerical investigation on a paraffin wax/graphene oxide/carbon nanotubes composite material for solar thermal storage applications. Appl Energy 2020;264:114786.
[2] Bashir MA, Daabo AM, Amber KP, Khan MS, Arshad A, Elahi H. Effect of phase change materials on the short-term thermal storage in the solar receiver of dish-micro gas turbine systems: A numerical analysis. Appl Therm Eng 2021;195:117179.
[3] Eisapour M, Eisapour AH, Hosseini MJ, Talebizadehsardari P. Exergy and energy analysis of wavy tubes photovoltaic-thermal systems using microencapsulated PCM nano-slurry coolant fluid. Appl Energy 2020;266:114849.
[4] Gao Y, Zheng Q, Jonsson JC, Lubner S, Curcija C, Fernandes L, et al. Parametric study of solid-solid translucent phase change materials in building windows. Appl Energy 2021;301:117467.
[5] Jin X, Zhang S, Xu X, Zhang X. Effects of PCM state on its phase change performance and the thermal performance of building walls. Build Environ 2014;81:334–9.
[6] Liu L, Zhang X, Liang H, Niu J, Wu J-Y. Cooling storage performance of a novel phase change material nano-emulsion for room air-conditioning in a self-designed pilot thermal storage unit. Appl Energy 2022;308:118405.
[7] Wang G, Yang Y, Wang S. Ocean thermal energy application technologies for unmanned underwater vehicles: A comprehensive review. Appl Energy 2020;278:115752.
[8] Arshad A, Jabbal M, Faraji H, Talebizadehsardari P, Bashir MA, Yan Y. Thermal performance of a phase change material-based heat sink in presence of nanoparticles and metal-foam to enhance cooling performance of electronics. J Storage Mater 2022;48:103882.
[9] Arshad A, Jabbal M, Shi L, Yan Y. Thermophysical characteristics and enhancement analysis of carbon-additives phase change mono and hybrid materials for thermal management of electronic devices. J Storage Mater 2021;34:102231.
[10] Jian-you L. Numerical and experimental investigation for heat transfer in triplex concentric tube with phase change material for thermal energy storage. Sol Energy 2008;82:977–85.
[11] Mahdi JM, Nsofor EC. Melting enhancement in triplex-tube latent thermal energy storage system using nanoparticles-fins combination. Int J Heat Mass Transf 2017;109:417–27.
[12] Al-Abidi AA, Mat S, Sopian K, Sulaiman MY, Mohammad AT. Numerical study of PCM solidification in a triplex tube heat exchanger with internal and external fins. Int J Heat Mass Transf 2013;61:684–95.
[13] Sharifi N, Faghri A, Bergman TL, Andraka CE. Simulation of heat pipe-assisted latent heat thermal energy storage with simultaneous charging and discharging. Int J Heat Mass Transf 2015;80:170–9.
[14] Arshad A, Jabbal M, Shi L, Darkwa J, Weston NJ, Yan Y. Development of TiO2/RT–35HC based nanocomposite phase change materials (NCPCMs) for thermal management applications. Sustainable Energy Technol Assess 2021;43:100865.
[15] Arshad A, Jabbal M, Yan Y. Preparation and characteristics evaluation of mono and hybrid nano-enhanced phase change materials (NePCMs) for thermal management of microelectronics. Energy Convers Manage 2020;205:112444.
[16] Han Y, Yang Y, Mallick T, Wen C. Nanoparticles to enhance melting performance of phase change materials for thermal energy storage. Nanomaterials 2022;12.
[17] Arshad A, Jabbal M, Yan Y. Thermal performance of PCM-based heat sink with partially filled copper oxide coated metal-foam for thermal management of microelectronics. In: 2020 19th IEEE intersociety conference on thermal and thermomechanical phenomena in electronic systems (ITherm); 2020. p. 697–702.
[18] Arshad A, Faraji H, Jabbal M, Yan Y. A numerical study of HNCPCM filled metal-foam strips based heat sink for passive cooling. In: 2021 20th IEEE intersociety conference on thermal and thermomechanical phenomena in electronic systems (iTherm); 2021. p. 524–30.
[19] Mahdi JM, Nsofor EC. Melting enhancement in triplex-tube latent heat energy storage system using nanoparticles-metal foam combination. Appl Energy 2017;191:22–34.
[20] Lal Rinawa M, Chauhan P, Sharma R, Poonia A, Kumar Singh H, Kumar Sharma A, et al. Numerical investigation of modified fin shapes for the improved heat transfer. Mater Today: Proc 2022;62:1854–60.
[21] Mahdi JM, Najim FT, Aljubury IMA, Mohammed HI, Khedher NB, Alshammari NK, et al. Intensifying the thermal response of PCM via fin-assisted foam strips in the shell-and-tube heat storage system. J Storage Mater 2022;45:103733.
[22] Luo X, Gu J, Ma H, Xie Y, Li A, Wang J, et al. Numerical study on enhanced melting heat transfer of PCM by the combined fractal fins. J Storage Mater 2022;45:103780.
[23] Zonouzi SA, Dadvar A. Numerical investigation of using helical fins for the enhancement of the charging process of a latent heat thermal energy storage system. J Storage Mater 2022;49:104157.
[24] Al-Mudhafar AHN, Nowakowski AF, Nicolleau FCGA. Enhancing the thermal performance of PCM in a shell and tube latent heat energy storage system by utilizing innovative fins. Energy Rep 2021;7:120–6.
[25] Wang G, Feng L, Altanji M, Sharma K, Sooppy Nisar K, khorasani S. Proposing novel "L" shaped fin to boost the melting performance of a vertical PCM enclosure. Case Studies in Thermal Engineering. 2021;28:101465.
[26] Zhang J, Cao Z, Huang S, Huang X, Liang K, Yang Y, et al. Improving the melting performance of phase change materials using novel fins and nanoparticles in tubular energy storage systems. Appl Energy 2022;322:119416.
[27] Yang Y, Zhu X, Ding H, Wen C. Performance of triangular finned triple tubes with phase change materials (PCMs) for thermal energy storage. In: Wen C, Yan Y, editors. Advances in heat transfer and thermal engineering. Singapore: Springer Singapore; 2021. p. 869–74.
[28] Sciacovelli A, Gagliardi F, Verda V. Maximization of performance of a PCM latent heat storage system with innovative fins. Appl Energy 2015;137:707–15.
[29] Mosaffa AH, Talati F, Basirat Tabrizi H, Rosen MA. Analytical modeling of PCM solidification in a shell and tube finned thermal storage for air conditioning systems. Energy Build 2012;49:356–61.
[30] Mazhar AR, Shukla A, Liu S. Numerical analysis of rectangular fins in a PCM for low-grade heat harnessing. Int J Therm Sci 2020;152:106306.
[31] Sheikholeslami M, Haq R-u, Shafee A, Li Z. Heat transfer behavior of nanoparticle enhanced PCM solidification through an enclosure with V shaped fins. Int J Heat Mass Transf 2019;130:1322–42.
[32] Deng S, Nie C, Wei G, Ye W-B. Improving the melting performance of a horizontal shell-tube latent-heat thermal energy storage unit using local enhanced finned tube. Energy Build 2019;183:161–73.
[33] Mahdi JM, Lohrasbi S, Ganji DD, Nsofor EC. Accelerated melting of PCM in energy storage systems via novel configuration of fins in the triplex-tube heat exchanger. Int J Heat Mass Transf 2018;124:663–76.
[34] Yao S, Huang X. Study on solidification performance of PCM by longitudinal triangular fins in a triplex-tube thermal energy storage system. Energy 2021;227:120527.
[35] Safari V, Abolghasemi H, Kamkari B. Experimental and numerical investigations of thermal performance enhancement in a latent heat storage heat exchanger using bifurcated and straight fins. Renewable Energy 2021;174:102–21.
[36] Safari V, Abolghasemi H, Darvishvand L, Kamkari B. Thermal performance investigation of concentric and eccentric shell and tube heat exchangers with different fin configurations containing phase change material. J Storage Mater 2021;37:102458.
[37] RT82, PCM RT-LINE Rubitherm Technologies GmbH - Imhoffweg 6 - 12307 Berlin.
[38] Bejan A, Lorente S. Constructal law of design and evolution: Physics, biology, technology, and society. J Appl Phys 2013;113:151301.
[39] Brent AD, Voller VR, Reid KJ. Enthalpy-porosity technique for modeling convection-diffusion phase change: application to the melting of a pure metal. Numerical Heat Transfer 1988;13:297–318.
[40] Yang X-H, Tan S-C, Liu J. Numerical investigation of the phase change process of low melting point metal. Int J Heat Mass Transf 2016;100:899–907.
[41] Al-Abidi AA, Mat S, Sopian K, Sulaiman MY, Mohammad AT. Experimental study of melting and solidification of PCM in a triplex tube heat exchanger with fins. Energy Build 2014;68:33–41.
[42] Ye W-B. Enhanced latent heat thermal energy storage in the double tubes using fins. J Therm Anal Calorim 2017;128:533–40.
[43] Ye W-B. Melting process in a rectangular thermal storage cavity heated from vertical walls. J Therm Analand Calorimetry 2016;123:873–80.
[44] Ye W-B, Guo H-J, Huang S-M, Hong Y-X. Research on melting and solidification processes for enhanced double tubes with constant wall temperature/wall heat flux. Heat Transfer—Asian Res. 2018;47:583–99.